

## Electronic supplementary information

### **Mediating in situ-generated fluorescence for Au nanocluster-based multi-color ratiometric detection of alkaline phosphatase**

Chao-Zhe Zhu<sup>a</sup>, Shuo Tian<sup>c</sup>, Hua-Nong Ting<sup>d</sup>, Mengke Wang<sup>c,\*</sup>, Yufeng Wang<sup>b,\*</sup>

a College of Medical Engineering, Jining Medical University, Jining, Shandong 272067, China

b School of Medical Information Engineering, Jining Medical University, Rizhao, Shandong 276826, China

c Nanozyme Laboratory in Zhongyuan, Henan Academy of Innovations in Medical Science, Zhengzhou, Henan 451163, China.

d Department of Biomedical Engineering, Faculty of Engineering, Universiti Malaya 50603 Kuala Lumpur, Malaysia

\*Corresponding author

E-mail address: wangmengke19@163.com; wyf@mail.jnmc.edu.cn

The conditions for the preparation of AuNCs were systematically optimized. As shown in **Fig. S1A**, the optimal reaction temperature was determined to be 70 °C. Furthermore, **Fig. S1B** demonstrates that the optimal reaction duration was 15 min. Additionally, **Fig. S1B** also indicates that the optimal BSA concentration was found to be 25.00 mg/mL.

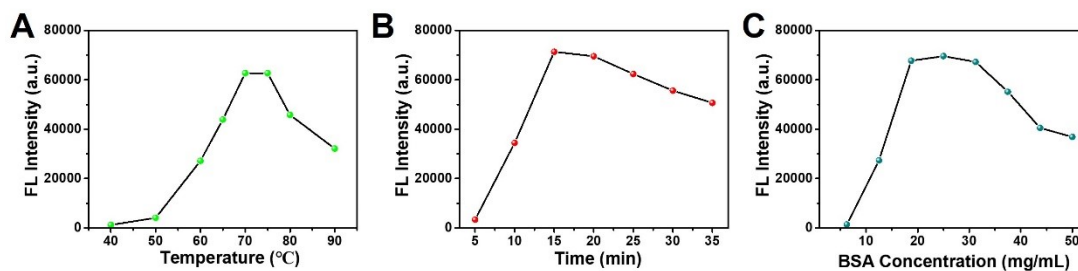


**Fig. S1** Synthesis optimization of AuNCs under varied (A) temperature, (B) time and (C) BSA concentration.

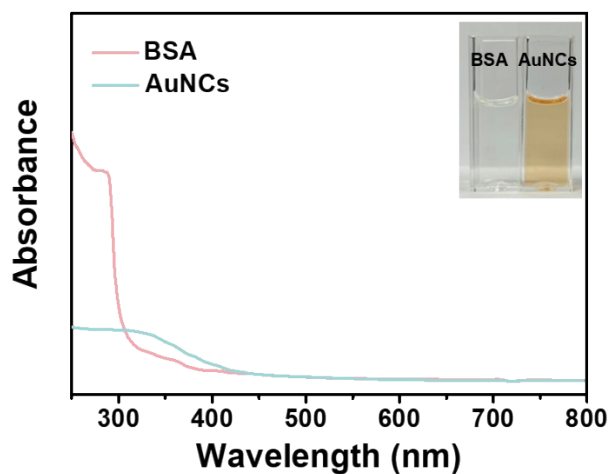


**Fig. S2** UV-vis absorption spectra of BSA and AuNCs.

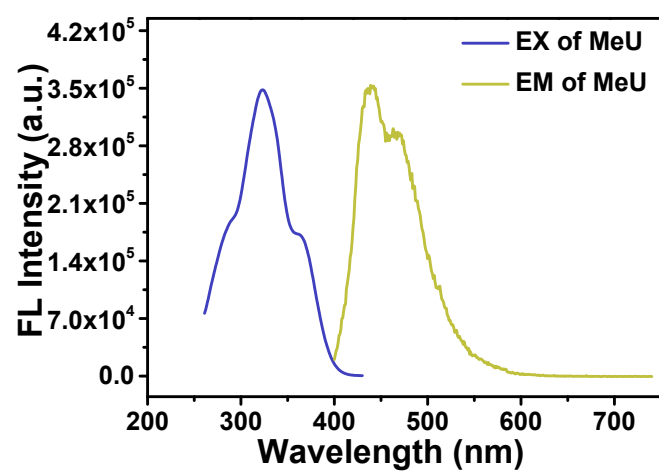


**Fig. S3** Fluorescence excitation and emission spectra of MeU.

To achieve high sensitivity, related factors of ALP enzymatic hydrolysis incubation pH, time and substrate MeUP concentration were investigated before the application for ALP activity analysis (Fig. S4A-C). From Fig. S4A and S4B, it can be observed that fluorescence intensity ratio of MeUP/ALP/AuNCs system obtained the maximum value at pH 9.0 and reaction time of 50 min. It can be seen that the fluorescence intensity ratio of MeUP/ALP/AuNCs system gradually increased with increasing MeUP concentration (Fig. S4C). As a result, the optimized conditions of enzymatic pH of 9.0, enzymatic incubation time of 50 min, MeUP concentration of 0.1 mM (55  $\mu$ L) were selected for the analysis of ALP activity.

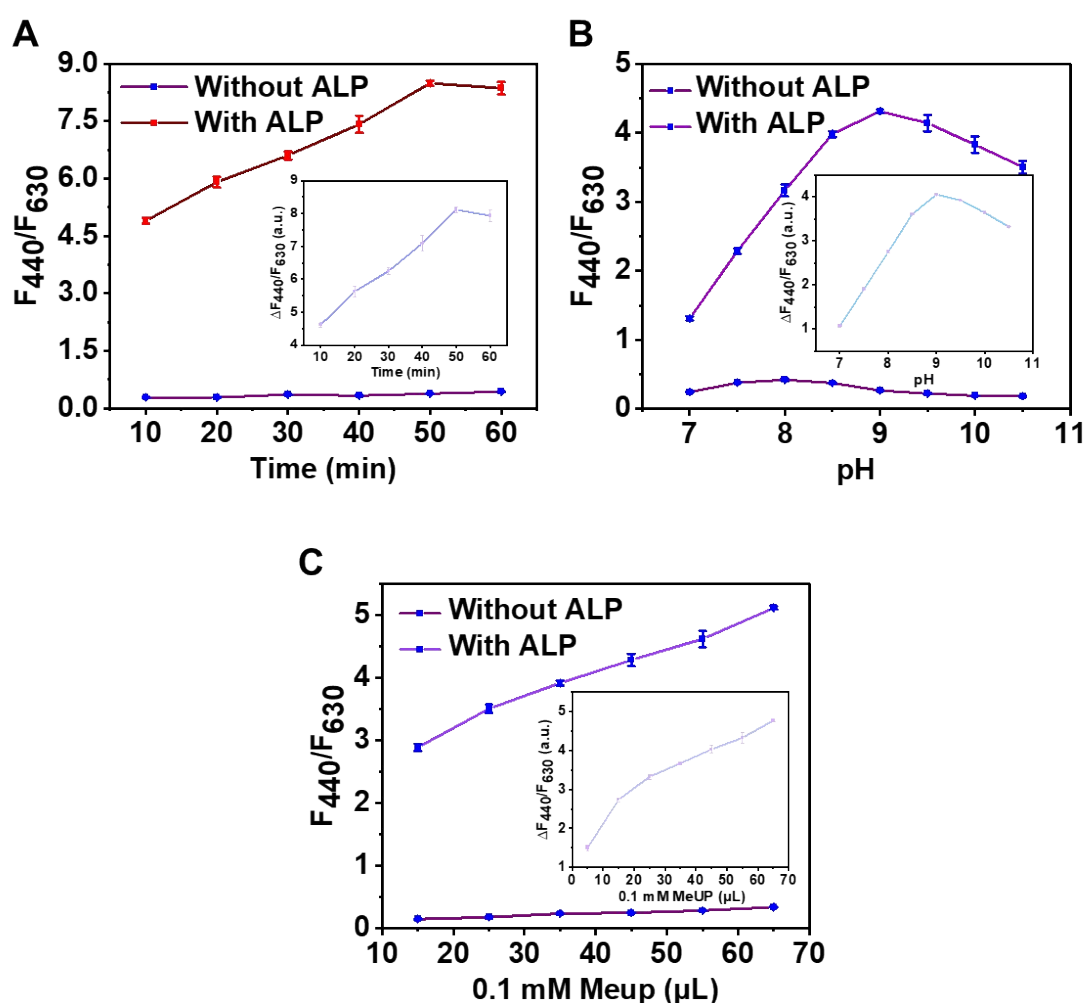


**Fig. S4** Effect of incubation (A) time, (B) pH, and (C) substrate MeUP concentration on the fluorescence intensity of MeUP/ALP/AuNCs system.

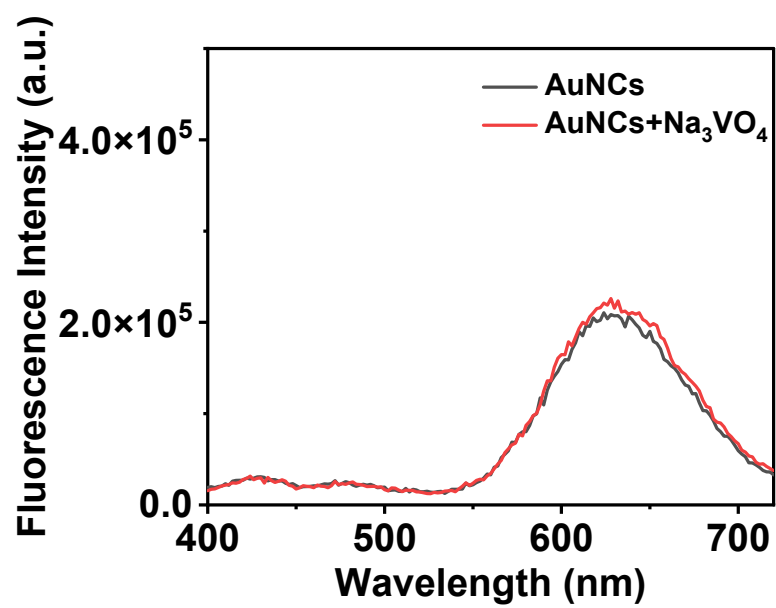


**Fig. S5** Fluorescence excitation and emission spectra of AuNCs and AuNCs/Na<sub>3</sub>VO<sub>4</sub>.

The enzymatic activity of ALP in human serum samples was quantified using a pNPP-based colorimetric method as previously reported<sup>1</sup>. This method relies on ALP-catalyzed hydrolysis of p-nitrophenyl phosphate (pNPP) to p-nitrophenol (pNP), which exhibits a characteristic absorption peak at 405 nm. For the assay, a reaction mixture containing ALP (60  $\mu$ L, activity gradient) and pNPP (140  $\mu$ L, 2.5 mM) was prepared in Tris-HCl buffer (100  $\mu$ L, 10 mM, pH 9.0), followed by incubation at 37  $^{\circ}$ C for 60 min. Subsequently, an additional 200  $\mu$ L of Tris-HCl buffer (10 mM, pH 9.0) was added to terminate the reaction. The absorbance spectra of the pNPP/ALP system were recorded using UV-vis spectroscopy (**Fig. S6A**). A calibration curve was established by plotting the net absorbance difference ( $\Delta A = A - A_0$ ), A and  $A_0$  represented the absorbance intensity at 405 nm of pNPP/ALP system in the presence and absence of ALP, against ALP activity (**Fig. S6B**). To validate clinical applicability, serum samples spiked with ALP were analyzed using this protocol, and the results demonstrated satisfactory recovery rates (**Table S3**).

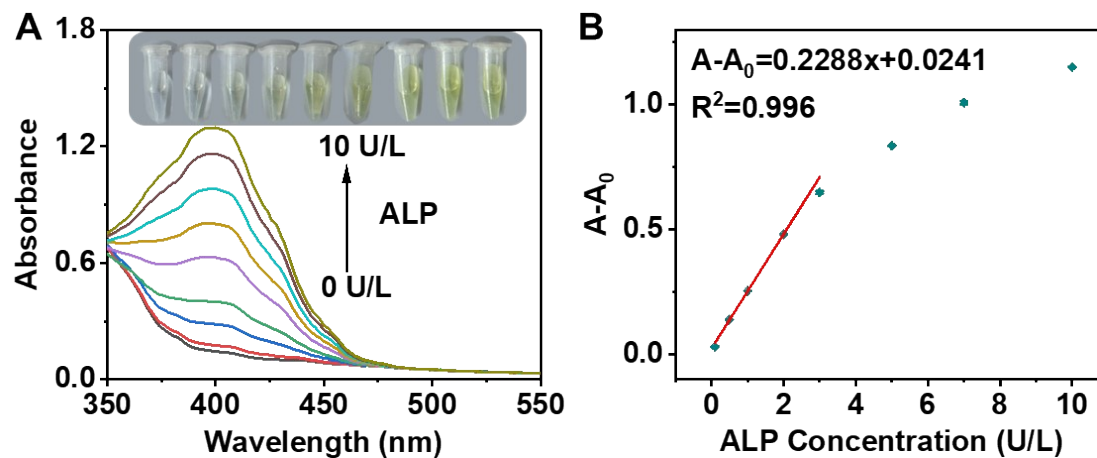


**Fig. S6** (A) UV-vis absorption spectra of the pNPP system after incubation with different amounts of ALP. (B) The plot of the difference absorbance at 405 nm ( $A - A_0$ , A and  $A_0$  represented the absorbance intensity at 405 nm of pNPP/ALP system in the presence and absence of ALP) versus ALP concentration.

**Table S1.** The corresponding CIE coordinates of MeUP/ALP/AuNCs system with varied ALP from 0 to 2.0 U/L.

ALP concentration (U/L)	CIE x	CIE y
0	0.45423	0.28742
0.007	0.33563	0.22191
0.01	0.30377	0.20383
0.02	0.25846	0.18163
0.05	0.22428	0.17001
0.1	0.20608	0.16608
0.2	0.19874	0.16811
0.4	0.1919	0.16666
0.6	0.18972	0.16729
0.8	0.1883	0.16635
1.0	0.1881	0.16692
1.5	0.18829	0.16727
2.0	0.18803	0.16771

**Table S2.** Comparison of different methods for the sensing of ALP activity.

Methods	System	Linear range (U/L)	LOD (U/L)	Ref.
Colorimetry	IOPM nanoparticle	0.05–40 U/L	0.045	2
Colorimetry	Mn-nanozyme	0.1-10	0.059	3
Colorimetry	Fluorescein	0.2-80	0.18	4
SERS	Fe <sub>3</sub> O <sub>4</sub> @Au@TiO <sub>2</sub>	2–10	1.17	5
SERS	Zn-MOFs	1-300	0.38	6
Electrochemistry	Hemin/G-quadruplex	0.1-5	0.03	7
Fluorescence	N-CQDs	5-360	1.1	8
Fluorescence	g-C <sub>3</sub> N <sub>4</sub> /CoOOH	1-30	0.92	9
Fluorescence	UCNPs/AgTNPs	0.06-12	0.035	10
Fluorescence	calcein–Ce <sup>3+</sup>	0-1.4	0.069	11
Fluorescence	CuNCs	0.5-25	0.15	12
Fluorescence	MoS <sub>2</sub> QDs	0.1-5	0.1	13
Fluorescence	NGQDs	0.1-5	0.07	14
Fluorescence	2,3-diaminonaphthalene	0.1-60	0.08	15
Fluorescence	CIP@SiO <sub>2</sub> -Ce/ATP-Tris	0.1–20	0.0025	16
Fluorescence	AuNCs@HDS	0.01-1.2 U/L	0.0092	17
Fluorescence	MeUP/AuNCs	0.007–0.6	0.0053	This work

1 **Table S3** Measurements of ALP in human serum samples.

Sample <sup>a</sup>	Determined (U L <sup>-1</sup> )			Added (U L <sup>-1</sup> )	This method			Hydrogel kit		
	This method	pNPP method	Hydrogel kit		Found (U L <sup>-1</sup> )	Recovery (%)	RSD (% n = 3)	Found (U L <sup>-1</sup> )	Recovery (%)	RSD (% n = 3)
1	0.16	0.18	0.19	0.15	0.32	106.7	3.21	0.33	93.3	4.02
				0.25	0.43	108.0	4.23	0.43	96.0	1.26
2	0.13	0.16	0.15	0.15	0.27	93.3	3.67	0.29	93.3	3.51
				0.25	0.39	104.0	4.18	0.41	104.0	2.21
3	0.27	0.25	0.23	0.15	0.41	93.3	1.32	0.39	106.7	4.98
				0.25	0.51	96.0	2.76	0.46	92.0	1.25

2 <sup>a</sup> Human serum sample was finally diluted 400-fold.

3 <sup>b</sup> The values was obtained by the pNPP-based method

## 1 Reference

1. P. Ni, C. Chen, Y. Jiang, C. Zhang, B. Wang, B. Cao, C. Li and Y. Lu, *Sensors and Actuators B: Chemical*, 2019, **301**, 127080.
2. Y. Gao, X. Gao, H. Hou, Z. Qu, H. Li, B. Du and P. Tang, *Sensors and Actuators B: Chemical*, 2024, **404**, 135280.
3. B. Wang, X. D. Zhang, G. Kang, F. N. Liu, D. Zhao, C. X. Chen and Y. Z. Lu, *Chinese Journal of Analytical Chemistry*, 2022, **50**, 54-63.
4. X. Hu, C. Sun, Y. Shi, Y. Long and H. Zheng, *New Journal of Chemistry*, 2019, **43**, 4525-4530.
5. J. Lie, F. Luo, Y. Liu, Y. Yang, Q. Nie, X. Chen, R. You, Y. Liu, X. Xiao and Y. Lu, *Chemical Engineering Journal*, 2024, **479**, 147241.
6. C. Y. Xi, M. Zhang, L. Jiang, H. Y. Chen, J. Lv, Y. He, M. E. Hafez, R. C. Qian and D. W. Li, *Sensors and Actuators B-Chemical*, 2022, **369**.
7. Y. Q. Liu, E. H. Xiong, X. Y. Li, J. J. Li, X. H. Zhang and J. H. Chen, *Biosensors & Bioelectronics*, 2017, **87**, 970-975.
8. F. Niu, Y.-L. Ying, X. Hua, Y. Niu, Y. Xu and Y.-T. Long, *Carbon*, 2018, **127**, 340-348.
9. S. G. Liu, L. Han, N. Li, Y. Z. Fan, Y. Z. Yang, N. B. Li and H. Q. Luo, *Sens. Actuator B-Chem.*, 2019, **283**, 515-523.
10. H. Y. Chen, X. Pang, Z. Q. Ni, M. L. Liu, Y. Y. Zhang and S. Z. Yao, *Analytica Chimica Acta*, 2020, **1095**, 146-153.
11. T. Feng, Y. Huang and S. Yan, *Analytical and Bioanalytical Chemistry*, 2024, **416**, 5317-5324.
12. F. Geng, C. Zou, J. Liu, Q. Zhang, X. Guo, Y. Fan, H. Yu, S. Yang, Z. Liu and L. Li, *Analytica Chimica Acta*, 2019, **1076**, 131-137.
13. Y. Zhong, F. Xue, P. Wei, R. Li, C. Cao and T. Yi, *Nanoscale*, 2018, **10**, 21298-21306.
14. J. Liu, D. Tang, Z. Chen, X. Yan, Z. Zhong, L. Kang and J. Yao, *Biosensors & Bioelectronics*, 2017, **94**, 271-277.
15. J. Wen, Y. Hu, N. Li, D. Li, G. Zheng, Y. Zou, M. Zhang and L. Shui, *Analytica Chimica*

- 1        *Acta*, 2022, **1230**, 340414.
- 2 16.    H. Yu, Z. Qiang, Y. Sun, M. Sun, L. Zhang, B. Yu, W. Lei and W. Zhang, *Analyst*, 2025,
- 3        **150**, 87-93.
- 4 17.    M. Wang, Y. Han, R. Huang, Z. Wang and G. Wang, *Sensors and Actuators B: Chemical*,
- 5        2024, **401**, 135038.